

# Linking the Structure and Thermal Stability of $\beta$ -Galactoside-Binding Protein Galectin-1 to Ligand Binding and Dimerization Equilibria<sup>†</sup>

Santiago Di Lella,<sup>‡</sup> Marcelo A. Martí,<sup>‡,§</sup> Diego O. Croci,<sup>||</sup> Carlos M. A. Guardia,<sup>‡</sup> Juan C. Díaz-Ricci,<sup>⊥</sup>  
Gabriel A. Rabinovich,<sup>§,||</sup> Julio J. Caramelo,<sup>§,@</sup> and Darío A. Estrin<sup>\*,‡</sup>

<sup>‡</sup>*Departamento de Química Inorgánica, Analítica y Química-Física (INQUIMAE-CONICET), and* <sup>§</sup>*Departamento de Química Biológica, Facultad de Ciencias Exactas y Naturales, Universidad de Buenos Aires, Ciudad de Buenos Aires, Argentina,* <sup>||</sup>*Laboratorio de Inmunopatología, Instituto de Biología y Medicina Experimental, CONICET, Ciudad de Buenos Aires, Argentina,* <sup>⊥</sup>*Instituto Superior de Investigaciones Biológicas, CONICET-Facultad de Bioquímica, Química y Farmacia, Universidad Nacional de Tucumán, San Miguel de Tucumán, Argentina, and* <sup>@</sup>*Fundación Instituto Leloir, Ciudad de Buenos Aires, Argentina*

Received March 9, 2010; Revised Manuscript Received July 16, 2010

**ABSTRACT:** The stability of proteins involves a critical balance of interactions of different orders of magnitude. In this work, we present experimental evidence of an increased thermal stability of galectin-1, a multi-functional  $\beta$ -galactoside-binding protein, upon binding to the disaccharide lactose. Analysis of structural changes occurring upon binding of lectin to its specific glycans and thermal denaturation of the protein and the complex were analyzed by circular dichroism. On the other hand, we studied dimerization as another factor that may induce structural and thermal stability changes. The results were then complemented with molecular dynamics simulations followed by a detailed computation of thermodynamic properties, including the internal energy, solvation free energy, and conformational entropy. In addition, an energetic profile of the binding and dimerization processes is also presented. Whereas binding and cross-linking of lactose do not alter galectin-1 structure, this interaction leads to substantial changes in the flexibility and internal energy of the protein which confers increased thermal stability to this endogenous lectin. Given that an improved understanding of the physicochemical properties of galectin–glycan lattices may contribute to the dissection of their biological functions and prediction of their therapeutic applications, our study suggests that galectin binding to specific disaccharide ligands may increase the thermal stability of this glycan-binding protein, an effect that could influence its critical biological functions.

The stability of a protein depends on the subtle balance between interactions and conformational dynamics taking place in the native state and those operating in the unfolded state of the molecule. The energetic and entropic contributions of these factors in both states are thousands of kilocalories per mole at room temperature, while the preference of the native state is in the 10 kcal/mol range, evidence of a subtle equilibrium (1). A number of parameters, such as pH, temperature, reducing conditions, oligomerization state, and ligand binding, may alter the balance of these interactions, leading to substantial modulation of protein stability (1, 2).

To accomplish their demanding tasks in living cells, proteins must interact specifically with other molecules, including lipids, nucleic acids, and carbohydrates, that in some cases significantly influence their stability (3). Recent studies clearly illustrated this concept as naturally glycosylated proteins in which polysaccharides are attached to specific amino acid side chains showed changes in their structural stability (4). Noncovalent interactions of proteins with small ligands may also result in enhanced protein thermal stability because of the coupling of binding and unfolding

equilibria (5–10). In general, as ligands bind preferentially to the native state of a protein, an increase in thermal stability due to ligand binding may represent simply an example of Le Chatelier's principle (11). In some cases, however, binding of the ligand alters the protein structure, with a concomitant additional increase in protein stability (12). An interesting case occurs when the increased stability induced by ligand binding decreases protein flexibility, because of a change in packing density. This decrease in protein flexibility is expected to result in an entropic penalty for the ligand-bound native state, increasing its free energy compared to that of the unfolded state (6). Although the thermodynamics of this process has been largely studied, it is still poorly understood.

Galectin-1 (Gal-1),<sup>1</sup> an evolutionarily conserved glycan-binding protein with specificity for *N*-acetylglucosamine-containing *N*- and *O*-glycans (Figure 1), is composed of 134 amino acids that coexist in a dynamic monomer–dimer equilibrium (13). This endogenous lectin has been proposed to play a key role in a broad spectrum of biological processes, including inflammation, immunity, neuronal processes, angiogenesis, and tumor progression (14). Probably, the most studied functions relate to the ability of this glycan-binding protein to control innate and adaptive immune cell homeostasis (15–17). Each monomer is

<sup>†</sup>This work was supported by grants from the University of Buenos Aires (Project X074) and from the Argentine National Science Agency (PICT Raíces 157 and PME 2006-1581). S.D.L. and C.M.A.G. are CONICET fellows. D.O.C. is a fellow from FONCYT. D.A.E., M.A.M., J.C.D.-R., J.J.C., and G.A.R. are researchers of CONICET.

\*To whom correspondence should be addressed. E-mail: dario@qi.fcen.uba.ar. Phone: +54 11 45763378, ext. 105. Fax: +54 11 45763348.

<sup>1</sup>Abbreviations: Gal-1, galectin-1; mGal-1, mutant monomeric galectin-1; dGal-1, dimeric galectin-1; CRD, carbohydrate recognition domain; MD, molecular dynamics; Lac, lactose; CD, circular dichroism; PB, Poisson–Boltzmann method; rmsf, root-mean-square fluctuation; rmsd, root-mean-square deviation.

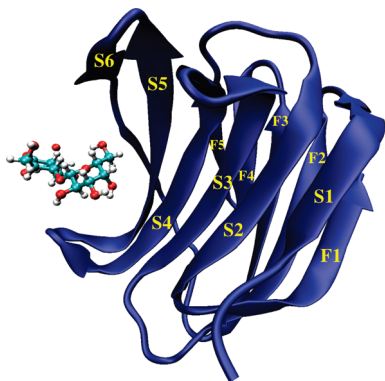


FIGURE 1: Representation of Gal-1 in its monomeric form, bound to the disaccharide lactose (Protein Data Bank entry 1W6O). Alpha-numeric labels indicate the six-strand sheet (S1–S6) and the five-strand sheet (F1–F5) composing the monomer structure.

arranged in a tightly folded conserved  $\beta$ -sandwich structure formed by a six-strand sheet (S1–S6) in the concave side where the ligand binds to a five-strand sheet (F1–F5) in the convex side (18). Gal-1 binds to its carbohydrate ligands through a conserved groove known as the carbohydrate recognition domain, corresponding to a region spanning amino acids 44–71. The main interactions, involving both hydrophobic and hydrogen bond networks, are established specifically by the residues histidine 44, asparagine 46, arginine 48, histidine 52, asparagine 61, tryptophan 68, glutamate 71, and arginine 73 (18, 19).

In addition to extensive analysis of its biological functions, galectin-1 has been extensively studied with regard to its glycan binding properties (18, 20–22). In fact, a recent study proposed that the galectin-1 monomer–dimer equilibrium can regulate the sensitivity of this lectin to oxidative inactivation, thus providing a mechanism whereby the ligand partially protects galectin-1 from oxidation, with critical effects on the functionality of this protein (23). Moreover, a number of studies have shown that oxidation of galectin-1 substantially alters its structure, an effect that is dependent on the oligomerization and binding state of the protein (19, 24). Taken together, these data suggest that galectin-1 dynamics may be substantially altered during the course of ligand binding and dimerization, yet the molecular basis underlying this process remains uncertain.

In this study, we analyzed the impact of ligand binding and dimerization on the structure and relative stability of galectin-1 by combining experimental and computer simulation-based approaches, namely, circular dichroism spectroscopy and molecular dynamics simulations. While experimental techniques allow a detailed characterization of the phenomenon, MD simulations provide a microscopic rational explanation for the observed effects.

## MATERIALS AND METHODS

**Preparation of Recombinant Gal-1.** Recombinant human Gal-1 was obtained as described previously (25). Briefly, *Escherichia coli* BL21(DE3) cells were transformed with a plasmid containing the *Lgals1* gene inserted into expression vector pET (Novagen), and production of recombinant Gal-1 was induced at the log phase by the addition of 1 mM isopropyl  $\beta$ -D-thiogalactoside. Cells were separated by centrifugation, washed, and disrupted by sonication. Debris was separated by centrifugation at 10000g, and soluble fractions were obtained for subsequent purification by affinity chromatography on a lactosyl-Sepharose column (Sigma-Aldrich).

The purification procedure was performed essentially as described previously (26). Because Gal-1 has unpaired cysteines in the binding site that can form intramolecular disulfide bonds in the absence of carbohydrate binding, reducing in this way its biological activity, we stored recombinant human Gal-1 in buffer containing 2-mercaptoethanol as described previously (27).

For all the experiments described below, Gal-1 was used at a concentration of 0.5 mg/mL in a 1  $\times$  PBS solution, which yields a protein concentration of 35  $\mu$ M in the samples. At this concentration, protein is expected to be in a dimeric form (21). Samples of Gal-1–Lac conjugate were prepared by addition of lactose to the medium to a final concentration of 10 mM. Considering the value of the Gal-1 affinity constant for lactose reported at room temperature ( $K_b = 3.25 \times 10^3 \text{ M}^{-1}$ ) (18), the lactose concentration used ensures that most of the protein stays in its bound state. As a negative control for experiments showing lactose bound to Gal-1, we used the non-galactosyl terminal disaccharide sucrose.

A similar protocol was adopted for the production of the N-Gal-1 mutant (mGal-1), which remains a monomer even at high concentrations (28).

**Circular Dichroism Spectroscopy.** Circular dichroism spectra were recorded using a Jasco J-815 spectropolarimeter equipped with a Peltier temperature control. Spectra were recorded using 1 mm path length polarimetrically certified cell (Hellma).

It is important to note here that the calculation of the  $T_m$  values for Gal-1 was dependent on initial conditions (incubation time and solution age). Nevertheless, the standard deviations for the calculated values were considerably small, and we will now focus on the change in  $T_m$  rather than in their absolute values.

**Molecular Dynamics Simulations.** Gal-1 coordinates were retrieved from Protein Data Bank entry 1W6N for the unbound protein (X-ray, 1.65 Å resolution) and entry 1W6O for the Gal-1–Lac complex. The C2S mutant (wild-type cysteine in position 2 replaced with a serine) was used, because of the availability of crystallographic data for the mutant protein and the mutant bound to different ligands (19, 20). In both cases, all crystallographic water molecules were deleted, and a single subunit was then solvated with three-site point charge modeled (TIP3P) water molecules in an octahedral box.

MD simulations were performed for both a single monomer and the dimer using the AMBER 9 (29) package of programs, with the PARM99 set of parameters (30) and the GLYCAM-04 parameters for carbohydrates (31).

The equilibration protocol consisted of performing 500-cycle runs of minimization to remove initial unfavorable contacts, followed by 100 ps simulations, during which systems were slowly heated from 0 K to the desired temperature of 300 K. The pressure was then equilibrated at 1 atm over 200 ps.

All simulations used the periodic boundary condition approximation and Ewald summation method with an 8 Å cutoff. The SHAKE algorithm was applied to all hydrogen-containing bonds. The MD simulations were performed at 300 K, using a 2 fs time step. All atoms in the simulated systems were allowed motional freedom. Snapshots of the coordinates were saved every 2 ps, over a total 50 ns of trajectory. The resulting 25000 instantaneous configurations saved on disk for each system were then analyzed.

**Calculation of Thermodynamic Parameters.** Thermodynamic parameters for both simulations were calculated using the MM\_PBSA approach, implemented in the AMBER 9 package (32). Energies were calculated from static decomposition of the MD

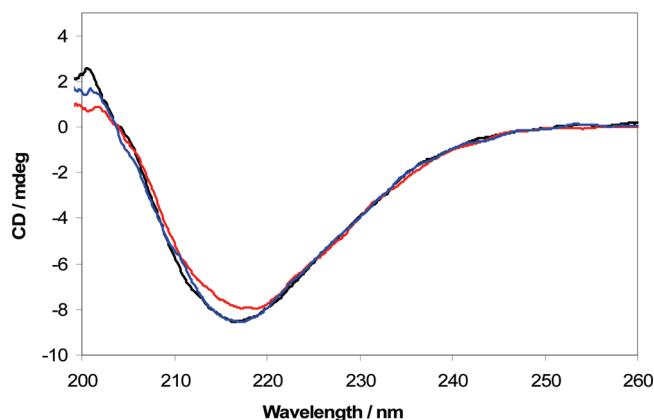


FIGURE 2: CD spectra of Gal-1 (black), the Gal-1-Lac complex (red), and Gal-1 in a sucrose solution (blue) at 298 K.

simulations of the complex, combining molecular mechanical energies with continuum solvent approaches. The molecular mechanical energies were determined with the *sander* program from AMBER and represented the internal energy (bond, angle, and dihedral) and van der Waals and electrostatic interactions (33). An infinite cutoff for all the interactions was used. The electrostatic contribution to the solvation free energy was calculated with a numerical solver for the Poisson-Boltzmann method (34, 35), as implemented in *sander* (32).

Conformational entropy calculations were performed by diagonalization of the Cartesian covariance matrix, by the methods of Schlitter (36) and Andricioaei and Karplus (37). Because the sampling in a molecular dynamics simulation depends on the length of the simulation, the calculated entropy also depends on the length of the trajectory used for the calculation. To obtain a value not depending on the trajectory length, we calculated the entropy for intervals ranging from 4 to 20 ns and fitted the entropy values to the following expression:

$$S(t) = S_{\infty} - \alpha/t^{2/3}$$

where  $S_{\infty}$  corresponds to the entropy when time approaches infinity and  $\alpha$  is an independent parameter. This procedure has been previously described by Harris et al. (38). For the calculations, we considered only the heavy atoms of all the amino acid residues of the protein, except three amino acid residues of both carboxyl- and amino-terminal regions. This last consideration was taken into account because of the high flexibility of the mentioned residues, as well as their localization far from the CRD.

## RESULTS

This section is organized as follows. First, experimental evidence based on CD spectroscopy is presented, showing the impact of lactose binding on Gal-1 structure and thermal stability. Second, equilibrium MD simulations of Gal-1 (both dimeric and monomeric forms) and the Gal-1-Lac complex are analyzed in association with microscopic changes induced by ligand binding and dimerization, followed by a comparative thermodynamic analysis of the corresponding Gal-1 states.

**Effects of Lactose Binding and Dimerization on Gal-1 Structure and Thermal Stability As Determined by Circular Dichroism.** We began the study of ligand binding effects on Gal-1 structure and thermal stability by measuring CD spectra of Gal-1 in different buffer solutions. The corresponding CD spectra at room temperature are shown in Figure 2.

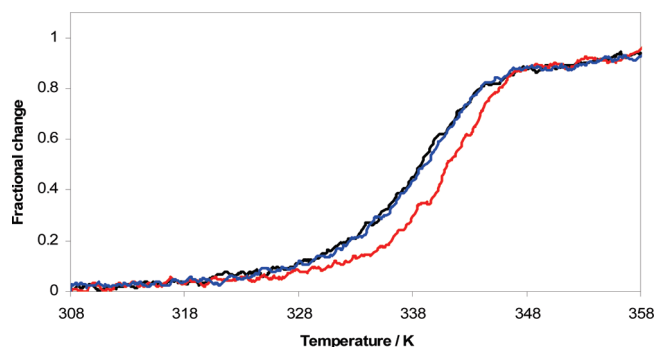


FIGURE 3: Fractional change in intensity of the 216 nm signal with respect to the incubation temperature of Gal-1 (black), the Gal-1-Lac complex (red), and Gal-1 in a sucrose solution (blue).

The general appearance of the Gal-1 spectrum is dominated by peptide secondary structures, with a broad and negative peak around 216 nm. The signals observed are indicative of  $\beta$ -sheet components (39), as expected for the Gal-1 secondary structure reported by X-ray crystallography (18). Similar overall spectra are observed for Gal-1 in buffer, Gal-1 in a 10 mM lactose solution, and Gal-1 in a 10 mM sucrose solution. Nevertheless, a more detailed inspection of the CD spectra reveals a slight difference in the intensity of the band for Gal-1 in a lactose solution when compared to buffer or sucrose solutions. This last fact may be indicative of the formation of the Gal-1-Lac complex, and a consequent subtle change in protein structure. Such a change is not observed in the spectrum for Gal-1 in a 10 mM sucrose solution, indicating that the difference may be attributable to the specific interaction between Gal-1 and its ligand, and not as a consequence of the presence of the carbohydrate in the buffer solution, which is known to alter solution properties, such as viscosity.

In a set of experiments, thermally induced structural perturbations were investigated for Gal-1 based on CD spectra. A typical perturbation protocol was adopted, consisting of successive incubations of the protein solution at increasing temperatures during the spectroscopic measurement. The apparent midpoint transition ( $T_m$ ) was defined as the temperature at which the intensity of the spectral feature falls to half of its initial value. The spectral feature measured here is the intensity of the band centered at 216 nm. Results are shown in Figure 3. The observed spectral changes are consistent with those expected for the melting of a  $\beta$ -sheet structure and the formation of an unfolded peptide, as previously reported (39, 40).

Further heating resulted in a more pronounced loss of secondary structure and a consequent decreased intensity for the band centered at 216 nm. Parameters were optimized by fitting the corresponding equation to the experimental data, leading to  $T_m$  values of 338 K for Gal-1 (or Gal-1 in a sucrose solution) and 341 K for Gal-1 in a lactose solution (standard deviation  $<0.2$  K).

To rule out the possibility that increased thermal stability could arise from a nonspecific effect exerted by the carbohydrate, we analyzed the effect of temperature on the Gal-1 structure when adding a non-galactosyl terminal sugar, such as sucrose. As shown in Figure 3, the calculated  $T_m$  derived from the curve upon addition of sucrose shows no effect on Gal-1 thermal stability, supporting the idea that the observed effect of lactose is in fact due to the specific binding to the lectin and not to the simple presence of a sugar in solution.



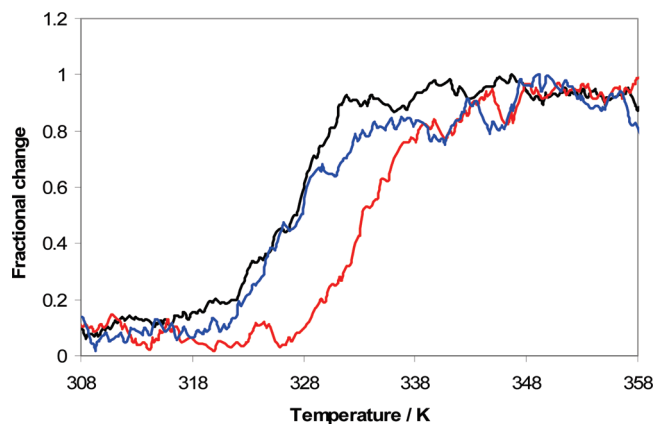


FIGURE 4: Fractional change in intensity of the 216 nm signal with respect to the incubation temperature of monomeric mGal-1 (black), the mGal-1–Lac complex (red), and mGal-1 in a sucrose solution (blue).

As mentioned in the introductory section, Gal-1 coexists in a monomer–dimer equilibrium. Therefore, and with the purpose of dissecting ligand binding from possible dimerization effects on Gal-1 CRD, we performed the same analysis for the monomeric Gal-1 (mGal-1). The corresponding results are shown in Figure 4. Adjustment of parameters after fitting the corresponding functions yields values of 327 and 333 K (standard deviation  $<0.7$  K) for mGal-1 and the mGal-1–Lac complex, respectively. Again, the addition of sucrose to the medium does not provide any difference with respect to the solution without it.

To test the reversibility of the thermal perturbation of the protein, we measured spectra after cooling the solutions to the reference temperature of 298 K. The spectrum at the high temperature reveals a lack of defined secondary structure, while the spectrum taken back to 298 K does not reproduce the original spectrum, revealing the irreversible nature of the thermal denaturation of the protein (data not shown).

**Analysis of Gal-1 and the Gal-1–Lac Complex by MD Simulations.** In search of an explanation for the observed increased thermal stability, and with the aim of providing microscopic insights into the structural changes that overcome to Gal-1 CRD upon ligand binding and dimerization, we performed MD simulations for both mGal-1 and the mGal-1–Lac complex, and for dimeric Gal-1. For each protein state, we performed a 50 ns equilibrium MD simulation. The root-mean-square deviation (rmsd) versus time plots for all systems (presented in the Supporting Information) show that after proper equilibration the systems remain stable during the time scale of our simulation. In addition, the rmsd for the ligand heavy atoms showed that for Gal-1–Lac complexes the carbohydrate remains in the same position during the whole simulation time.

To analyze the effect of lactose binding on mGal-1 dynamics and flexibility, we first computed the root-mean-square fluctuation (rmsf) versus residue plot for both mGal-1 and mGal-1–Lac ensembles. Results are shown in Figure 5.

As shown by the plots depicted in Figure 5, the overall flexibility of the protein is low ( $<2$  Å) in most regions and similar in both cases, which may be taken as an indication that the general flexibility of the protein remained unchanged upon ligand binding. Although the *B* factor values in the Protein Data Bank files would be indicative of flexibility, in the cases being studied, crystal packing effects may be responsible for the lack of significant differences for the desired analysis.

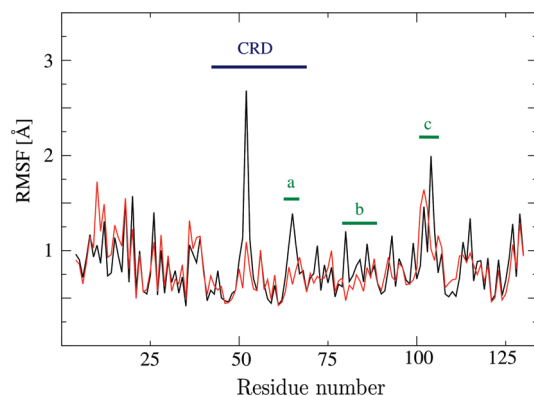


FIGURE 5: Root-mean-square fluctuations (rmsf) per amino acid residue considering all heavy atoms, of both mGal-1 (black) and the mGal-1–Lac complex (red), for the total simulation time. The last three residues of the amino and carboxyl termini are not shown. Regions with high variation between both traces are denoted as follows: CRD, carbohydrate recognition domain; a,  $\beta$ -turn between strands S5 and S6 (residues 62–65); b, unordered region between strands S6 and F3 (residues 77–81); c,  $\beta$ -turn between strands F3 and F4 (residues 101–103).

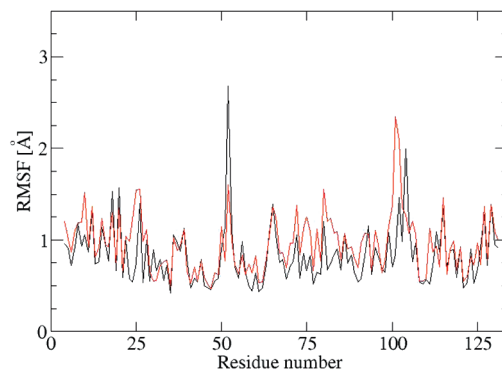


FIGURE 6: Root-mean-square fluctuations (rmsf) per amino acid residue considering all heavy atoms, of both mGal-1 (black) and dGal-1 (red), for the total simulation time. The last three residues of the amino and carboxyl termini are not shown.

There are, however, some particular regions where the mGal-1–Lac complex has a significantly reduced mobility. These correspond to the Gal-1 CRD (amino acids 44–73), a  $\beta$ -turn between strands S5 and S6 (residues 62–65), an unordered region between strands S6 and F3 (residues 77–81), and the  $\beta$ -turn between strands F3 and F4 (residues 101–103), better shown in the protein structure representation in Figure 1. All these regions exhibited significantly reduced fluctuations when lactose bound to the protein (Figure 5). Interestingly, these regions are all located in or near the ligand binding groove of the protein, which is the region involved in the binding of the saccharide. Also, particularly interesting was the significant change in the rmsf of histidine 52. The reason for the latter is the change in the side chain flexibility of the His involved in ligand binding (shown in the Supporting Information). The ring flipping was frequent in the unbound state, while in the ligand-bound condition, just a few flipping events were observed.

Thus, while only minor changes are observed in the whole rmsf, a loss of flexibility is mainly observed in this restricted area.

We now analyze the rmsf of dimeric Gal-1 compared to that of monomeric mGal-1 (Figure 6). Because in the dimer two monomers are simulated, in the presented rmsf versus residue number plot the average values between both monomers in the dimer

Table 1: Thermodynamic Parameters Calculated for Formation of the Complex during Ligand Binding (CF) or Dimerization (dim)<sup>a</sup>

	$\Delta E_{\text{assoc}}$	$\Delta G_{\text{assoc}}^{\text{PB}}$	$\Delta S$
$\Delta_{\text{CF}}$	-76.6	52.1	-45.9
$\Delta_{\text{dim}}$	-291.8	229.9	19.5

<sup>a</sup> $\Delta E_{\text{assoc}}$  and  $\Delta G_{\text{assoc}}^{\text{PB}}$  are the differences in internal energy and solvation free energy, respectively, for the association of Gal-1 with ligand or the other monomer.  $\Delta S$  is the change in entropy in a CRD subunit due to each considered process. All energy values are in kilocalories per mole, and entropy values are in calories per mole per kelvin.

structure are computed. As is evident in the plot, the rmsf values for both systems present small but noticeable differences. In general, regions corresponding to the loops are more flexible in both systems. It is clear that the dimer structure is more flexible in the regions corresponding to the  $\beta$ -turn between strands F3 and F4 (residues 101–103) and the unordered region between strands S6 and F3 (residues 77–81). On the other hand, the mGal-1 structure presents a slightly increased flexibility for amino acids 51–54, which is the region involved in the recognition.

**Calculation of Thermodynamic Parameters of Gal-1 and the Gal-1–Lac Complex.** To perform a thermodynamic analysis of Gal-1 thermal stability in the presence or absence of its specific ligand, and in the monomeric and dimeric form, we computed the total potential energy and solvation free energy of Gal-1 CRD in each state using MM\_PBSA, a continuum solvent model implemented in Amber (32). Because of the nature of the methodology employed, the total potential energy of each Gal-1 CRD system measures the internal interaction energy of the protein considering as reference a system in which the nonbonded interactions are measured with respect to isolated, quite separated atoms along with strains in angles and bonds due to the adoption of a given conformation. Even if the value itself has no physical meaning, as will be shown below, comparison of values for the same system (the CRD of Gal-1) in different situations (bound states and oligomeric forms) is meaningful.

To analyze both the ligand binding and dimerization processes in detail, we computed for each case (a) the intermolecular interaction  $\Delta E_{\text{assoc}}$  energy between the Gal-1 and lactose ( $\Delta_{\text{CF}}$ ) in the complex or between the two monomers in the dimer ( $\Delta_{\text{dim}}$ ) and (b) the change in the solvation free energy as a consequence of Gal-1–Lac association or formation of the Gal-1 dimer. We should note hereby that the values calculated may be overestimated, a common flaw of the MM\_PBSA method.

Finally, in search of an approximation to analyze the corresponding entropic change due to the presence of lactose binding to the CRD of Gal-1 ( $\Delta S_{\text{CF}}$ ) or as a consequence of dimer formation ( $\Delta S_{\text{dim}}$ ), we performed entropy calculations for each system as presented in Materials and Methods. Computed results are presented in Table 1.

Results listed in Table 1 show that ligand binding is energetically driven. The cost of desolvating a highly hydrophilic surface brings an important negative contribution to the solvation free energy. However, this is overcompensated by the tight interaction between a carbohydrate and a hydrophilic surface in the protein. Interestingly, upon binding, the protein loses conformational entropy (negative  $\Delta S$ ), since as expected from the previous results, the binding of lactose to Gal-1 reduces protein flexibility. Taken together, these results clearly show that ligand binding stabilizes Gal-1 due to intermolecular interactions, overcompensating for the entropic reduction, as well as the increase in solvation free energy.

Table 2: Melting Temperatures Obtained Experimentally of Unbound Gal-1 in the Dimeric (dGal-1) and Monomeric (mGal-1) Forms and Gal-1–Lac Complexes

system	$T_m$ (K)	system	$T_m$ (K)
dGal-1	338	mGal-1	327
dGal-1–Lac	341	mGal-1–Lac	333

When we switch to the parameters calculated for the dimerization process, it is evident that such a phenomenon is also energetically driven. In this case, there is a large energetic (both electrostatic and van der Waals components) contribution for the system due to association of both monomers. This last contribution is responsible for the protein existing preferentially as a dimer under physiological conditions. Nevertheless, a large change in solvation energy is observed, as shown by a Poisson–Boltzmann approximation for the association process. This issue may be rationalized due to occlusion of a large amphiphilic surface (most amino acids belonging to strands F1 and S1 participating in the dimeric interface) that needs to be desolvated to allow the dimer to be formed. With regard to the conformational entropy change in the dimerization process species, it is surprisingly positive, showing that CRD has more conformational freedom in the dimer state, consistent with the rmsf results presented above.

## DISCUSSION

**Thermal Stability of Gal-1 and Ligand Binding.** The spectroscopic results show that Gal-1 is considerably stabilized by the presence of lactose and as a consequence of dimerization as shown by the obtained  $T_m$  values summarized in Table 2.

CD spectra showed that although both ligand binding and dimerization have a modest perturbation effect on Gal-1 CRD structure, both processes lead to increased thermal stability.

More interestingly, the stabilization provided by ligand binding and dimerization is additive to some extent, because different increases in  $T_m$  are observed for wild-type Gal-1 compared to the Gal-1 monomer mutant. Dimerization produces the largest 11 K increase in  $T_m$ , only minorly reduced (to 8 K) by the presence of bound lactose. Ligand binding on its own increases  $T_m$  by 6 K in the monomer and 3 K in the dimer. While not drastic, the effect of ligand binding on the  $T_m$  for both systems is still significant; similar results have been observed in other biomolecules (41–43). Results of experimental binding measurements have been previously provided for Gal-1 (18). However, those reported values correspond to the binding process as a whole, and not to the change in energy and entropy in the protein itself due to ligand binding or dimerization. The data, consistent with our simulation, show that ligand binding is enthalpically driven and a relatively large entropic cost is paid.

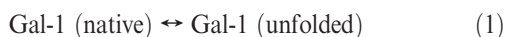
Both dimerization and ligand binding effects, taken together, increase the  $T_m$  by 14 K. The incomplete additivity of the dimerization and binding effect on Gal-1 CRD structure may point toward a partial overlap of the stabilization mechanism.

Another interesting issue involves the difference observed in the temperature range over which denaturation occurs. A detailed examination of Figures 3 and 4 makes evident the fact that mGal-1 undergoes structural changes while being heated in a temperature interval lower than that observed for wild-type Gal-1, mainly starting in the dimeric state. This may point to a different possible more complex unfolding mechanism in the dimer compared to that of mGal-1.

On the other hand, the curves for Gal-1 (Figure 3) do not appear to show any change in such a temperature range upon ligand binding, whereas the ones for mGal-1 in Figure 4 denote a slightly smaller temperature range for the change in structure for Gal-1 than for the Gal-1–Lac complex.

All these last observations may be indicative of an increased degree of cooperativity in the protein for the unfolding effect for the case of mGal-1, while the process was not remarkably altered in the case of dimeric Gal-1.

**Thermodynamic Analysis of the Association among Ligand Binding, Dimerization, and Unfolding Processes.** A subsequent qualitative thermodynamic analysis allows a physicochemical rationalization of the observed stabilization and provides a direct relationship among the measured  $T_m$  values. The unfolding process can be described assuming a simple two-state model:



The relation between the unfolding transition and the temperature can be described as

$$\Delta G_U = \Delta E_U - T\Delta S_U = (E_U - E_N) - T(S_U - S_N) \quad (2)$$

where  $\Delta G_U$ ,  $\Delta E_U$ , and  $\Delta S_U$  are the changes in free energy, internal energy, and entropy upon unfolding, respectively,  $T$  is the temperature of the system,  $E_U$  and  $S_U$  are the energy and entropy of the unfolded state, respectively, and  $E_N$  and  $S_N$  are the energy and entropy of the native state, respectively.

Taking mGal-1 as a reference system (from now on denoted with a degree symbol), one can now analyze how ligand binding and dimerization equilibria lead into an increase in  $T_m$ . The thermodynamics can be described by equations in the Supporting Information, leading to the following expression:

$$\Delta T = \frac{-(\Delta E - T_m^\circ \Delta S)}{\Delta S_U^\circ - \Delta S} \quad (3)$$

which relates the change in energy and entropy provided by the ligand binding (or dimerization) process to the change in  $T_m$ ,  $\Delta T$ .

Analysis of the equation shows that the denominator must always be positive, because  $\Delta S_U^\circ$  is the gain in entropy due to unfolding in the unbound state and  $\Delta S$  is the change in entropy due to ligand binding (or dimerization), which is always negative. Therefore, the sign and magnitude of the change in  $T_m$  will be given by the numerator. In a careful look at the expression, we can recognize that it is in fact the free energy of ligand dissociation at  $T = T_m^\circ$  (or  $-1 \times \Delta G$ ), but to observe an increase in  $T_m$  due to ligand binding, ligand must be bound at  $T_m^\circ$ ; therefore, the dissociation free energy must be positive at this temperature. In fact, if  $\Delta G$  at  $T_m^\circ$  equals zero, ligand dissociation and unfolding would happen together, resulting in  $T_m(L) = T_m^\circ$ . Consequently, to observe an increase in  $T_m$  due to ligand binding, the energetic balance between the energy gained due to formation of the protein ligand complex ( $\Delta E$ ), and the energy per degree due to  $\Delta S$ , must be big enough to allow a negative  $\Delta G(T_m^\circ)$ . Moreover, a small  $\Delta S$  will also favor a larger  $\Delta T$  by reducing the lower term in eq 3.

The thermodynamic data obtained from the MD simulations may help to understand this effect. Results presented in Table 1 show that, although there is a reduction in the protein conformational entropy, these changes are overcompensated mostly by energy of interaction due to protein ligand binding,  $\Delta E_{\text{assoc}}$ .

On the other hand, for the dimer it is evident that  $\Delta E_{\text{assoc}}$  is also responsible for overcompensating the large loss in solvation free energy. The small but still favorable entropy term also favors the dimer, all resulting in a more negative change in free energy and favoring the greater increase in  $T_m$ , as observed.

**Physiopathological Implications.** By recognizing multiple *N*-acetylglucosamine units on *N*- and *O*-glycans on the surface of immune, inflammatory, and neoplastic cells, Gal-1 triggers distinct biological events, including apoptosis, immunosuppression, and cell migration (14). Under this complex scenario, defining and characterizing the physicochemical parameters regulating binding of Gal-1 to its specific disaccharide lactose is of great importance for improving our understanding of the biological effects of this endogenous lectin at the crossroads of physiology and pathology. Moreover, understanding the biochemical and biophysical aspects of Gal-1 either free or complexed to specific disaccharides may contribute to the design of novel glycomimetics capable of interfering in Gal-1–glycan interactions during tumor escape and metastasis.

## CONCLUSION

In this work, we conducted an extensive analysis of the changes occurring in terms of Gal-1 structure, dynamics, and thermodynamics upon binding to the specific disaccharide lactose. Experimental results indicate the presence of the saccharide ligand does not alter the protein structure, although it certainly increases its thermal stability. While ligand binding to Gal-1 decreases considerably its flexibility and, therefore, the entropy of the protein and yields a negative difference in the solvation free energy of the protein, these changes are overridden by the energy gained upon complexation.

## ACKNOWLEDGMENT

We thank Dr. L. Baum for providing plasmids for the monomeric N-Gal-1 mutant. S.D.L. is indebted to Luciana Capece for her substantial help on simulations. MD simulations were performed in the CECAR, FCEN-UBA.

## SUPPORTING INFORMATION AVAILABLE

rmsd values for the molecular dynamics simulations performed in this study, a histogram showing the dihedral fluctuation of histidine 52, and the component contributions and standard deviation for data presented in Table 1. This material is available free of charge via the Internet at <http://pubs.acs.org>.

## REFERENCES

1. Fersht, A. (1998) *Structure and Mechanism in Protein Science. A Guide to Enzyme Catalysis and Protein Folding*, 1st ed., W. H. Freeman, New York.
2. Branden, C., and Tooze, J. (1991) *Introduction to protein structure*, Garland Publishing, Inc., New York.
3. Pace, C. N., Treviño, S., Prabhakaran, E., and Scholtz, J. M. (2004) Protein structure, stability and solubility in water and other solvents. *Philos. Trans. R. Soc. London, Ser. B* 359, 1225–1235.
4. Wang, C., Eufemi, M., Turano, C., and Giartosio, A. (1996) Influence of the Carbohydrate Moiety on the Stability of Glycoproteins. *Biochemistry* 35, 23.
5. Latypov, R. F., Liu, D., Gunasekaran, K., Harvey, T. S., Razinkov, V. I., and Raibekas, A. A. (2008) Structural and thermodynamic effects of ANS binding to human interleukin-1 receptor antagonist. *Protein Sci.* 17, 652–663.
6. Celej, M. S., Montich, G. G., and Fidelio, G. (2003) Protein stability induced by ligand binding correlates with changes in protein flexibility. *Protein Sci.* 12, 1496–1506.



7. Fukada, H., Sturtevant, J. M., and Quijcho, F. A. (1983) Thermodynamics of binding of L-arabinose and of D-galactose to the binding protein of *Escherichia coli*. *J. Biol. Chem.* 258, 13193–13198.
8. Brandts, J. F., and Lin, L.-N. (1990) Study of strong and ultratight protein interaction using differential scanning calorimetry. *Biochemistry* 29, 6927–6940.
9. Shrake, A., and Ross, P. D. (1990) Ligand-induced biphasic protein denaturation. *J. Biol. Chem.* 265, 5055–5059.
10. Shrake, A., and Ross, P. D. (1992) Origin and consequences of ligand-induced multiphasic thermal protein denaturation. *Biopolymers* 32, 925–940.
11. Celej, M. S., Montich, G. G., and Fidelio, G. (2004) Conformational flexibility of avidin: The influence of biotin binding. *Biochem. Biophys. Res. Commun.* 325, 922–927.
12. Kamerzell, T. J., Unruh, J. R., Johnson, C. K., and Middaugh, C. R. (2006) Conformational flexibility, hydration and state parameter fluctuations of fibroblast growth factor-10: Effects of ligand binding. *Biochemistry* 45 (51), 15288–15300.
13. Cooper, D. N. W., and Barondes, S. H. (1999) God must love galectins: He made so many of them. *Glycobiology* 9 (10), 979–984.
14. Yang, R. Y., Rabinovich, G. A., and Liu, F. T. (2008) Galectins: Structure, function and therapeutic potential. *Expert Rev. Mol. Med.* 10, e17.
15. Toscano, M., Bianco, G. A., Ilarregui, J. M., Croci, D. O., Correale, J., Hernandez, J. D., Zwirner, N. W., Poirier, F., Riley, E. M., Baum, L. G., and Rabinovich, G. A. (2007) Differential glycosylation of TH1, TH2 and TH-17 effector cells selectively regulates susceptibility to cell death. *Nat. Immunol.* 8 (8), 825–834.
16. Rabinovich, G. A., and Toscano, M. (2009) Turning “sweet” on immunity: Galectin-glycan interactions in immune tolerance and inflammation. *Nat. Rev. Immunol.* 9 (5), 338–352.
17. Ilarregui, J. M., Croci, D. O., Bianco, G. A., Toscano, M., Salatino, M., Vermeulen, M. E., Greffner, J. R., and Rabinovich, G. A. (2009) Tolerogenic signals delivered by dendritic cells to T cells through a galectin-1 driven immunoregulatory circuit involving interleukin 27 and interleukin 10. *Nat. Immunol.* 10 (9), 981–991.
18. Lopez-Lucendo, M. F., Solis, D., Andre, S., Hirabayashi, J., Kasai, K., Kaltner, H., Gabius, H. J., and Romero, A. (2004) Growth-regulatory human galectin-1: Crystallographic characterisation of the structural changes induced by single-site mutations and their impact on the thermodynamics of ligand binding. *J. Mol. Biol.* 343 (4), 957–970.
19. Ford, M. G., Weimar, T., Köhli, T., and Woods, R. J. (2003) Molecular Dynamics Simulations of Galectin-1-oligosaccharides Complexes Reveal the Molecular Basis of Ligand Diversity. *Proteins: Struct., Funct., Genet.* 53, 229–240.
20. Di Lella, S., Marti, M. A., Alvarez, R. M. S., Estrin, D. A., and Díaz Ricci, J. C. (2007) Characterization of the Carbohydrate Recognition Domain of Galectin-1 in Terms of Solvent Occupancy. *J. Phys. Chem. B* 111, 7360–7366.
21. Cho, M., and Cummings, R. D. (1995) Galectin-1, a  $\beta$ -galactoside-binding lectin in Chinese hamster ovary cells. I. Physical and chemical characterization. *J. Biol. Chem.* 270 (10), 5198–5206.
22. Ahmad, N., Gabius, H., Sabesan, S., Oscarson, S., and Brewer, C. F. (2004) Thermodynamic binding studies of bivalent oligosaccharides to galectin-1, galectin-3, and the carbohydrate recognition domain of galectin-3. *Glycobiology* 14 (9), 817–825.
23. Stowell, S. R., Cho, M., Feasley, C. L., Arthur, C. M., Song, X., Colucci, J. K., Karmakar, S., Mehta, P., Dias-Baruffi, M., McEver, R. P., and Cummings, R. D. (2009) Ligand reduces galectin-1 sensitivity to oxidative inactivation by enhancing dimer formation. *J. Biol. Chem.* 284 (8), 4989–4999.
24. Scott, K., and Weinberg, C. (2004) Galectin-1: A bifunctional regulator of cellular proliferation. *Glycoconjugate J.* 19 (7–9), 467–477.
25. Hirabayashi, J., Hashidate, T., Arata, Y., Nishi, N., Nakamura, T., Hirashima, M., Urashima, T., Oka, T., Futai, M., and Muller, W. E. (2002) Oligosaccharide specificity of galectins: A search by frontal affinity chromatography. *Biochim. Biophys. Acta* 1572, 232–254.
26. Barrionuevo, P., Beigier-Bompadre, M., Ilarregui, J. M., Toscano, M., Bianco, G. A., Isturiz, M. A., and Rabinovich, G. A. (2007) A novel function for galectin-1 at the crossroad of innate and adaptive immunity: Galectin-1 regulates monocyte/macrophage physiology through a nonapoptotic ERK-dependent pathway. *J. Immunol.* 178 (1), 436–445.
27. Pace, K. E., Hahn, H. P., and Baum, L. G. (2003) Preparation of recombinant human galectin-1 and use in T cell death assays. *Methods Enzymol.* 363, 499–518.
28. Cho, M., and Cummings, R. D. (1996) Characterization of monomeric forms of galectin-1 generated by site-directed mutagenesis. *Biochemistry* 35, 13081–13088.
29. Case, D. A., Darden, T. A., Cheatham, T. E., III, Simmerling, C. L., Wang, J., Duke, R. E., Luo, R., Merz, D. M., Wang, B., Pearlman, D. A., Crowley, M., Brozell, S., Tsui, V., Gohlke, H., Mongan, J., Hornak, V., Cui, G., Beroza, P., Schafmeister, C., Caldwell, J. W., Ross, W. S., and Kollman, P. A. (2004) AMBER 8, University of California, San Francisco.
30. Cheatham, T. E., Cieplak, P., and Kollman, P. A. (1999) A modified version of the Cornell et al. force field with improved sugar pucker phases and helical repeat. *J. Biomol. Struct. Dyn.* 16, 845–862.
31. Kirschner, K. N., and Woods, R. J. (2001) Solvent interactions determine carbohydrate conformation. *Proc. Natl. Acad. Sci. U.S.A.* 98 (19), 10541–10545.
32. Case, D. A., Darden, T. A., Cheatham, T. E., Simmerling, C., Wang, J., Duke, R. E., Luo, R., Merz, D. M., Pearlman, D. A., Crowley, M., Walker, R. C., Zhang, W., Wang, B., Hayik, S., Roitberg, A., Seabra, G., Wong, K. F., Paesani, F., Wu, X., Brozell, S., Tsui, V., Gohlke, H., Yang, L., Tan, C., Mongan, J., Hornak, V., Cui, G., Beroza, P., Mathews, D. H., Schafmeister, C., Ross, W. S., and Kollman, P. A. (2006) AMBER 9, University of California, San Francisco.
33. Case, D. A., Cheatham, T. E., Darden, T. A., Gohlke, H., Luo, R., Merz, K. M. J., Onufriev, A., Simmerling, C., Wang, B., and Woods, R. J. (2005) The Amber biomolecular simulation programs. *J. Comput. Chem.* 26, 1668–1688.
34. Constanciel, R., and Contreras, R. (1984) Self-Consistent Field-Theory of Solvent Effects Representation by Continuum Models: Introduction of Desolvation Contribution. *Theor. Chim. Acta* 65, 1–11.
35. Still, W. C., Tempczyk, A., Hawley, R. C., and Hendrickson, T. (1990) Semianalytical Treatment of Solvation for Molecular Mechanics and Dynamics. *J. Am. Chem. Soc.* 112, 6127–6129.
36. Schlitter, J. (1993) Estimation of absolute and relative entropies of macromolecules using the covariance matrix. *Chem. Phys. Lett.* 215, 617–621.
37. Andricioaei, I., and Karplus, M. (2001) On the calculation of entropy from covariance matrices of the atomic fluctuations. *J. Chem. Phys.* 115 (14), 6289–6292.
38. Harris, S. A., Gavathiotis, E., Searle, M. S., Orozco, M., and Laughton, C. A. (2001) Cooperativity in drug-DNA recognition: A molecular dynamics study. *J. Am. Chem. Soc.* 123, 12658–12663.
39. Lee Whitmore, B. A. W. (2008) Protein secondary structure analyses from circular dichroism spectroscopy: Methods and reference databases. *Biopolymers* 89 (5), 392–400.
40. Charalambous, K., O'Reilly, A. O., Bullough, P., and Wallace, B. A. (2009) Thermal and chemical unfolding and refolding of a eukaryotic sodium channel. *Biochim. Biophys. Acta* 1788, 1279–1286.
41. Waldron, T. T., and Murphy, K. P. (2003) Stabilization of Proteins by Ligand Binding: Application to Drug Screening and Determination of Unfolding Energetics. *Biochemistry* 42, 5058–5064.
42. Todorovic, S., Leal, S. S., Salgueiro, C. A., Zebger, I., Hildebrandt, P., Murgida, D. H., and Gomes, C. M. (2007) A Spectroscopic Study of the Temperature Induced Modifications on Ferredoxin Folding and Iron-Sulfur Moieties. *Biochemistry* 46, 10733–10738.
43. Matulis, D., Kranz, J. K., Salemme, F. R., and Todd, M. J. (2005) Thermodynamic Stability of Carbonic Anhydrase: Measurements of Binding Affinity and Stoichiometry Using ThermoFluor. *Biochemistry* 44, 5258–5266.